

Supporting Information

Enhanced Electrocatalytic overall water splitting performance of Ni-Re Thin Film alloy interface via Electrochemically Induced Lattice Strain

**Muthukrishnan Alagesan^{1,2}, Mathankumar Mahendran^{1,2}, Manickam
Pandiaraj^{1,2}, N Rajasekaran^{1,2*}**

*¹Academy of Scientific and Innovative Research (AcSIR), Ghaziabad-
201002, India,*

*²CSIR-Central Electrochemical Research Institute (CECRI), Karaikudi-
630003, Tamil Nadu, India.*

This file contains 27 pages in which Experimental section with electrochemical and structural characterisation procedure, SEM, XRD, XPS, FESEM and electrochemical results are provided along with CVs recorded in non-faradaic region with the calculation of TOF.

Experimental Section:

Chemical Reagents:

Nickel sulphate hexahydrate ($\text{NiSO}_4 \cdot 6\text{H}_2\text{O}$, 99%) was purchased from Fischer scientific, Potassium perrhenate (KReO_4 , 99%) was bought from Sigma Aldrich, Citric Acid Anhydrous ($\text{C}_6\text{H}_8\text{O}_7$, 99.5%) were purchased from SRL, and Ammonium Chloride (NH_4Cl) were RANKEM. Sodium Hydroxide (NaOH) Sodium carbonate (Na_2CO_3) was also purchased from SRL. Sulphuric Acid (H_2SO_4 , LR) was bought from Qualigens. Potassium Hydroxide (KOH) was also purchased from Fischer scientific which is used for electrolyte. 1M KOH is prepared by using Millipore water produced by a specialized water purification system.

Pre-treatment and Fabrication of Nickel-Rhenium alloy:

A copper sheet (0.5mm thickness) was used as a substrate and a nickel bar is used as an anode. In the pre-treatment process, copper substrates undergo an alkaline electro-cleaning process consisting of sodium hydroxide (3.5 wt%), sodium carbonate (2.5 wt%) with a current density of 20 A/dm^2 for 3 mins followed by an acid dipping process (30 v.% H_2SO_4). The electrode is washed using deionized water between each alkaline and acid cleaning. After that electrodeposition is carried out on two electrode systems in a double-walled cylindrical cell (to maintain the constant temperature) at a temperature of 50 °C. Electrodeposition was done by using 0.3 M Nickel sulphate, 0.01 M Potassium perrhenate, 0.3 M Citric acid, 0.15 M Ammonium chloride and 0.05 M Sodium saccharin dissolved in 100 mL of milli-pore water. Ni-Re catalyst was deposited at an area of 5 cm^2 ($2 \times 2.5 \text{ cm}^2$) carried out by varying current densities as 4 to 12 A/dm^2 at a constant pH of 5 and at a constant time interval of 15 minutes.

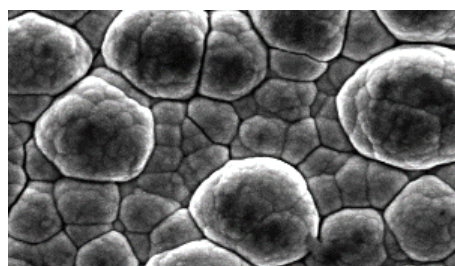
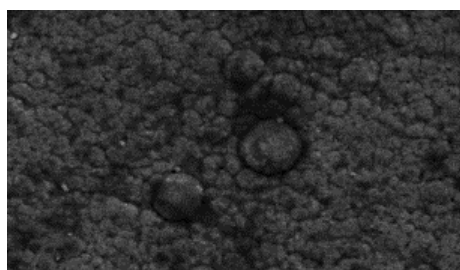
Electrochemical Characterization:

All electrochemical experiments were performed in a three-electrode cell electrochemical workstation (Metrohm Autolab instrument) at room temperature. Here Hg/HgO in 1M KOH is used as the reference electrode, the Graphite rod is used as the counter electrode and the fabricated Ni-Re electrodes are used as a working electrode. Where the overall performance of the prepared electrode was analysed by using 1M KOH electrolyte. Polarization curves (LSV) were studied at a sweep rate of 5 mV/s and 100 % iR compensation was done. The Tafel curves are obtained from the corresponding LSV curves at low current densities. Electrochemical impedance spectroscopy (EIS)

curves were also studied to check the charge transfer kinetics. Double-layer capacitance was measured from the electrochemical surface area (ECSA) and Turnover frequency was also calculated. The stability study of fabricated electrodes for both HER and OER studies and full cell studies was measured using potentiostatic (PSTAT) analysis for 24hrs without any iR compensation.

Structural Characterization:

All electrochemical experiments were subjected to three-electrode cell electrochemical workstation (Metrohm Autolab instrument) at room temperature. Morphology of the fabricated electrode is subjected to scanning electron microscope (SEM, TESCAN VEGA 3 SBH) and field emission scanning electron microscope (FESEM, Carl Zeiss, SUPRA 55VP) equipped with energy dispersive X-ray analysis (EDAX, BrukerEasy). Crystallinity and phase formation of the catalyst is examined by X-ray diffractometer (XRD, D8 Advance Bruker). Elemental composition and oxidation state of the catalyst is subjected to X-ray photoelectron spectrometer (XPS, Multilab 2000 Thermo Scientific). Microstructures, SAED pattern and lattice fringes of the electrode is equipped by High-resolution transmission electron microscopy (HR-TEM, FEI Tecnai G2 F20).



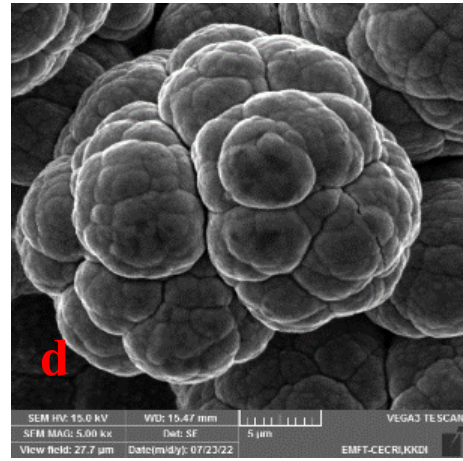
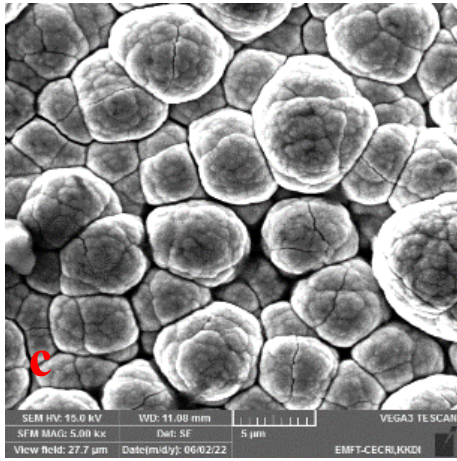
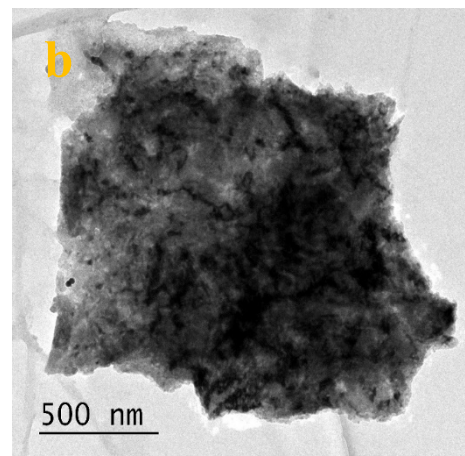
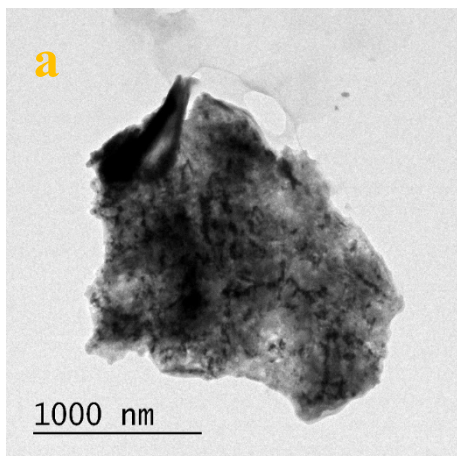


Fig.S1 (a-d) Different surface morphology of various Ni-Re alloy electrodeposited at various current densities.



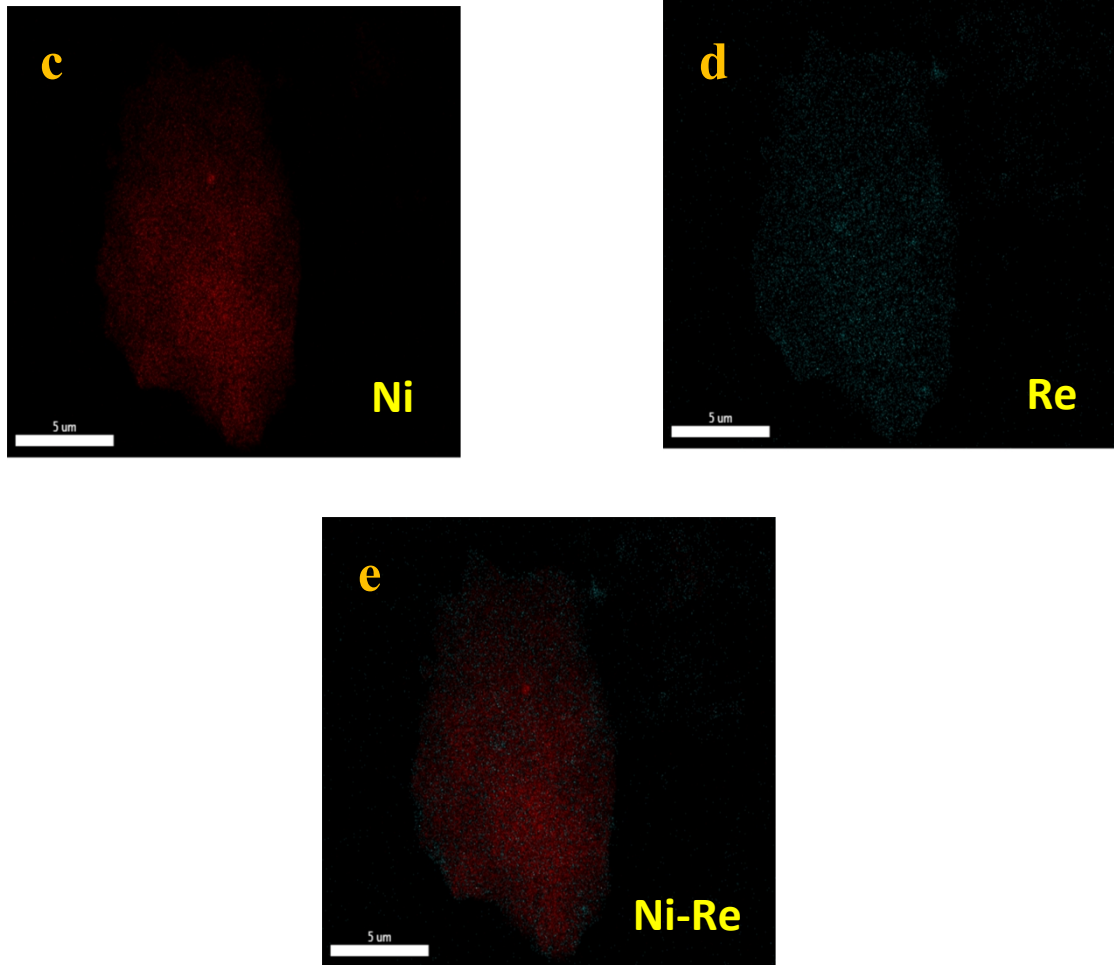


Figure S2 (a&b) High and low magnification of HR-TEM images of NR₁₅ alloy. Color mapping of (c) Nickel, (d) Rhenium, (e) Ni-Re alloy.

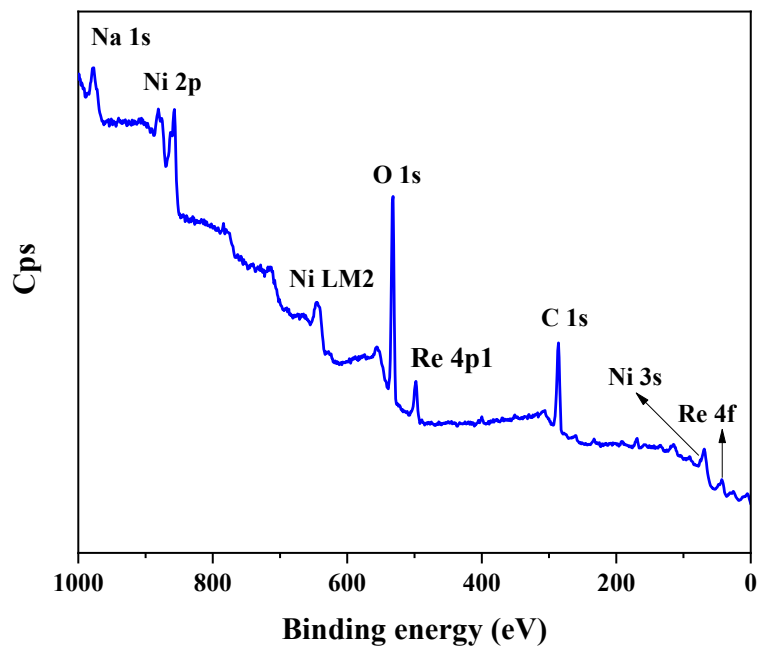


Fig. S3 XPS survey spectra of NR₁₅ alloy before activation.

PSTAT activation of all HER catalysts:

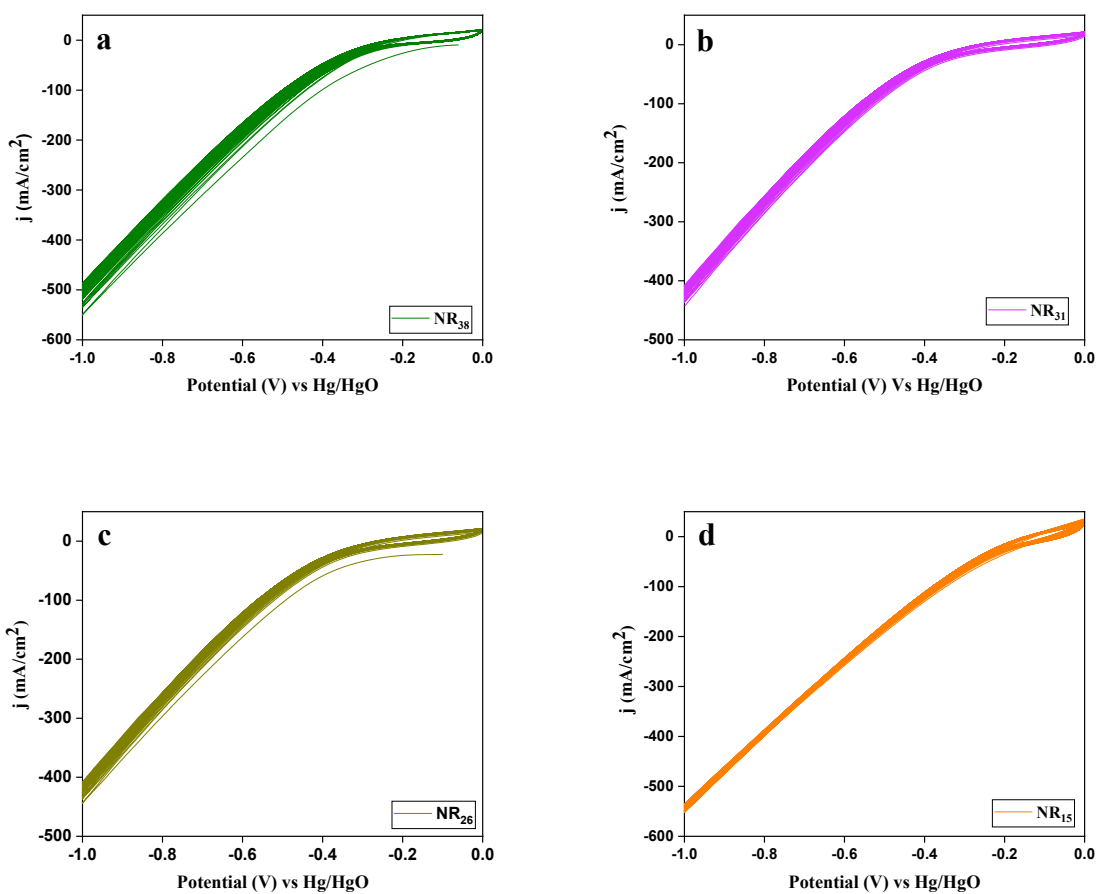


Fig.S4 The electrochemical activation of HER was performed on all the deposits using cyclic voltammetry with 500 cycles for all catalysts (a) NR₃₈ (b) NR₃₁, (c) NR₂₆, (d) NR₁₅.

PSTAT activation of all OER catalysts:

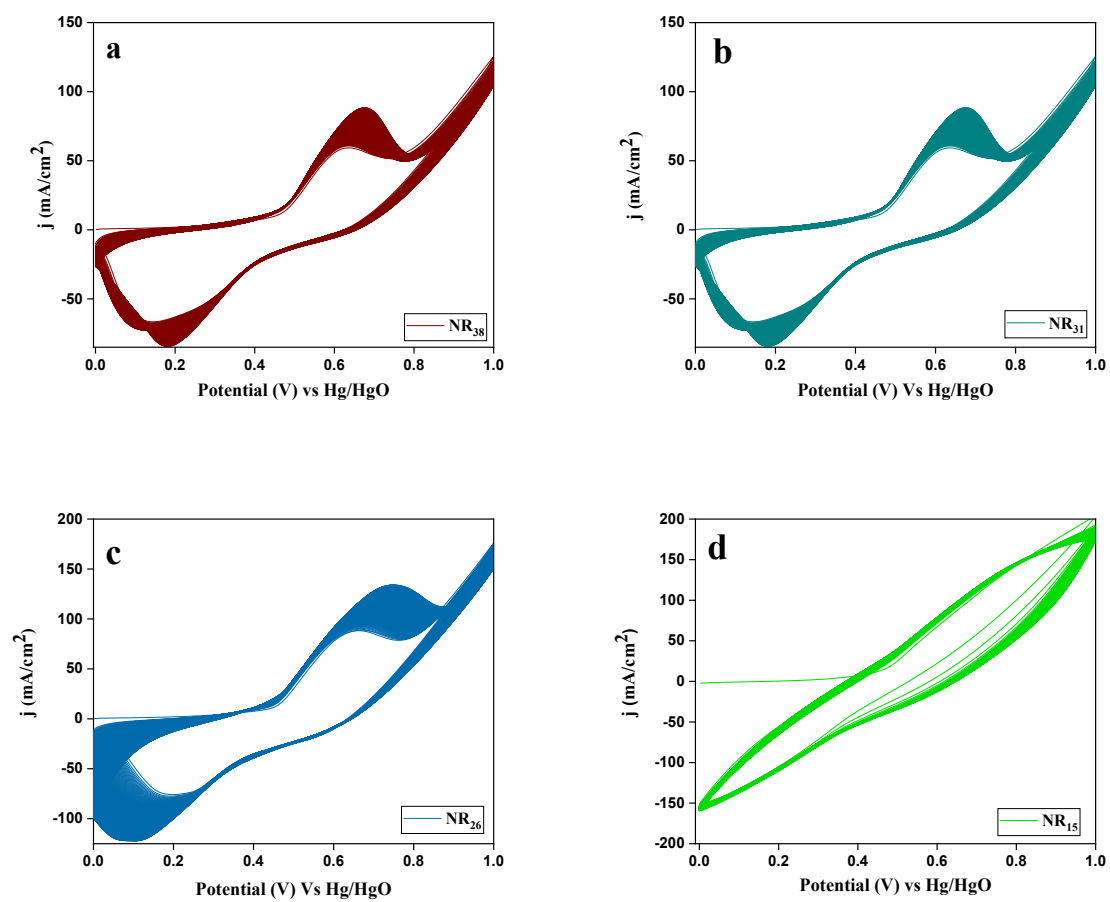


Fig.S5 The electrochemical activation of OER was performed on all the deposits using cyclic voltammetry with 500 cycles for all catalysts (a) NR₃₈ (b) NR₃₁, (c) NR₂₆, (d) NR₁₅.

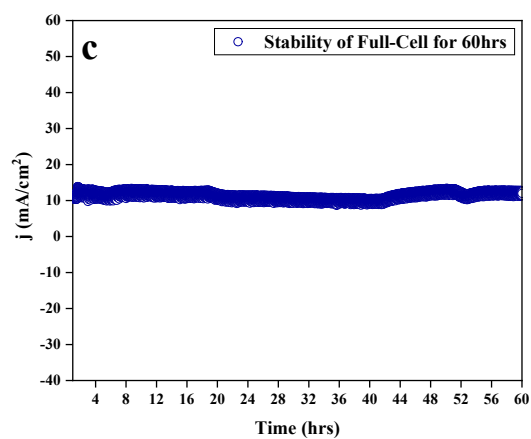
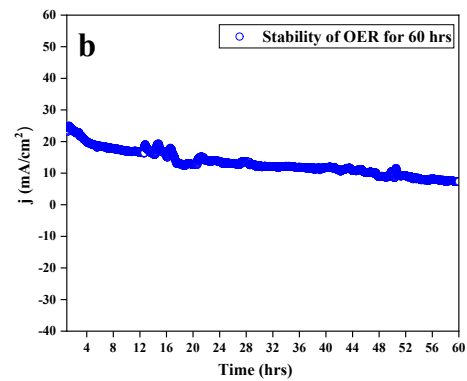
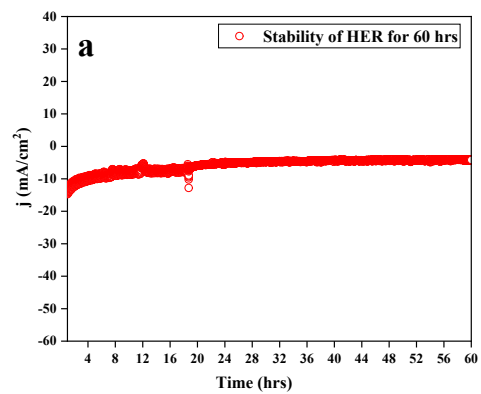


Fig.S6 (a) Stability studies of HER studies for 60 hrs, (b) Stability studies of OER studies for 60 hrs, (c) Stability studies of full cell studies for 60 hrs

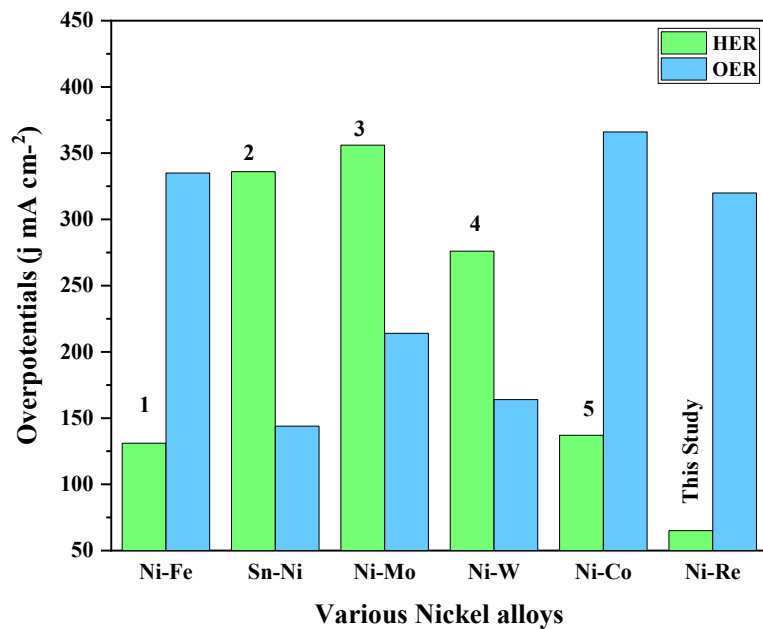


Fig.S7 Overpotentials of nickel-based alloys for HER and Studies.¹⁻⁵

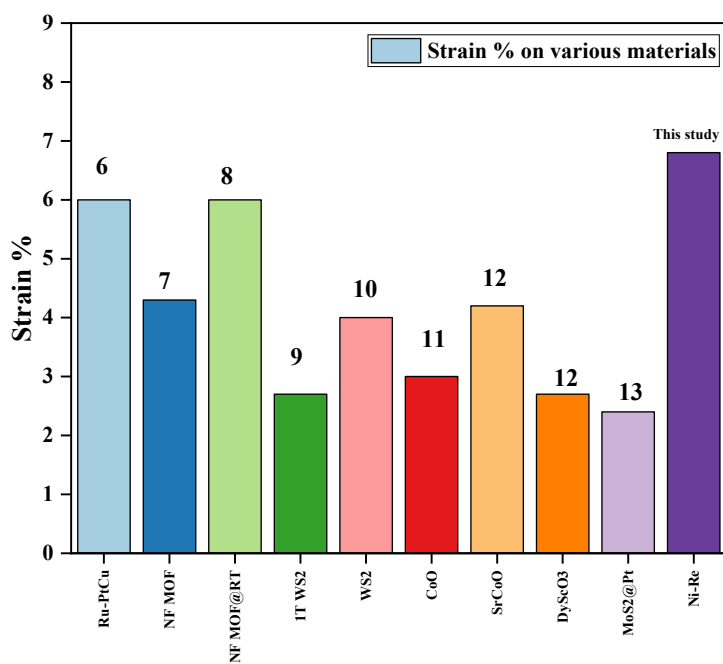
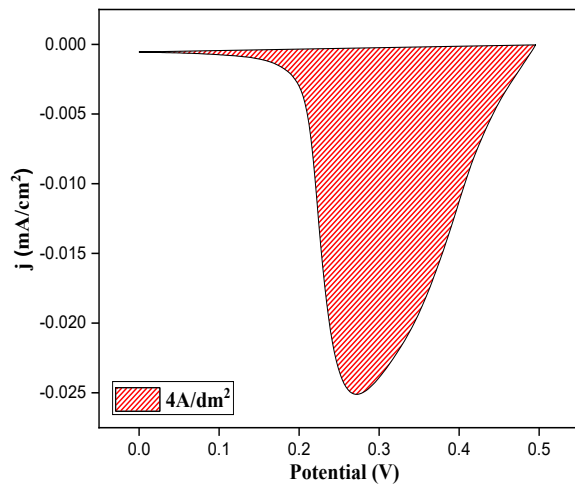


Fig.S8 Effect of Strain inducing into the various electrocatalysts.⁶⁻¹³

Fig.S9:

Determining Surface concentration from the redox curves of CV's of before activation:

i) $4A/dm^2$



S.A-0.00351VA

• **Calculation:**

$$\text{Calculated area} = 0.00351VA$$

$$\text{The associated charge is} = 0.00351 / 0.06Vs^{-1}$$

$$= 0.0585As$$

$$= 0.0585 C$$

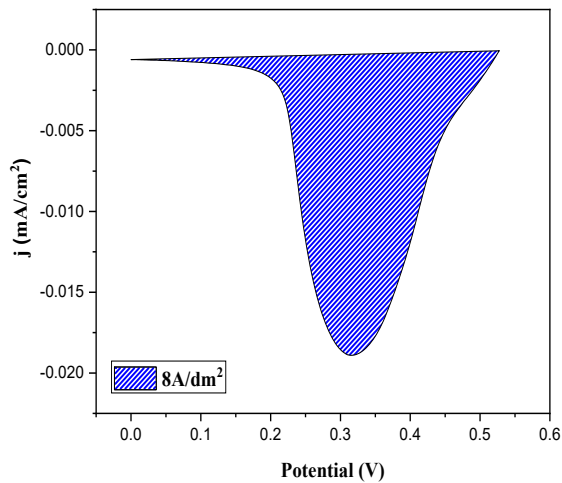
$$\text{The number of electron transferred is} = 0.0585C / 1.602 \times 10^{-19}$$

$$= 36.52 \times 10^{16}$$

Hence,

The surface concentration of Ni-Re participated in OER is $= 36.52 \times 10^{16}$ atoms

ii) $8\text{A}/\text{dm}^2$



S.A-0.00439VA

• **Calculation:**

$$\text{Calculated area} = 0.00439\text{VA}$$

$$\text{The associated charge is} = 0.00439 / 0.06\text{Vs}^{-1}$$

$$= 0.0732 \text{ As}$$

$$= 0.0732 \text{ C}$$

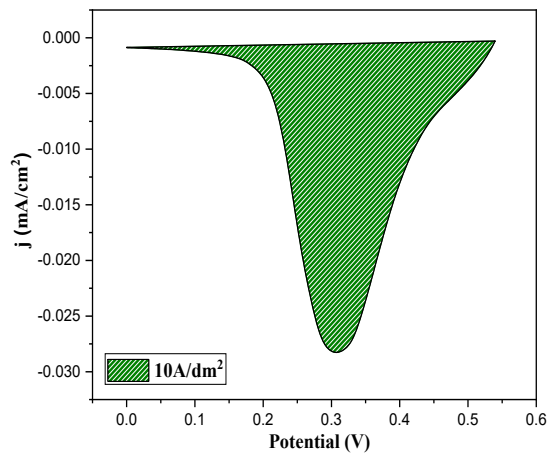
$$\text{The number of electron transferred is} = 0.0732\text{C} / 1.602 \times 10^{-19}$$

$$= 45.69 \times 10^{16}$$

Hence,

The surface concentration of Ni-Re participated in OER is $= 45.69 \times 10^{16}$ atoms.

iii) $10\text{A}/\text{dm}^2$:



S.A-0.00502VA

• **Calculation:**

$$\text{Calculated area} = 0.00502\text{VA}$$

$$\text{The associated charge is} = 0.00502 / 0.06\text{Vs}^{-1}$$

$$= 0.0837 \text{ As}$$

$$= 0.0837 \text{ C}$$

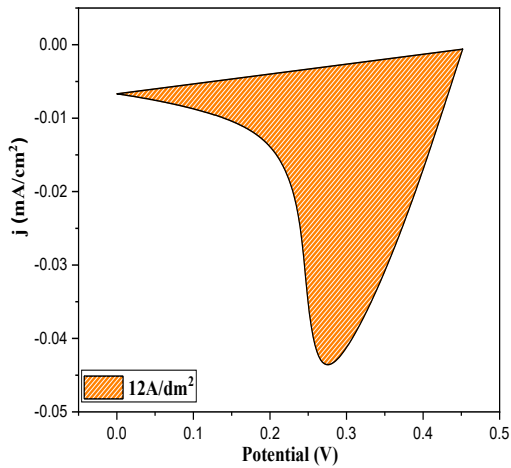
$$\text{The number of electron transferred is} = 0.0837\text{C} / 1.602 \times 10^{-19}$$

$$= 52.25 \times 10^{16}$$

Hence,

The surface concentration of Ni-Re participated in OER is $= 52.25 \times 10^{16}$ atoms.

iv) $12\text{A}/\text{dm}^2$:



S.A-0.00843VA

• **Calculation:**

Calculated area = 0.00843VA

The associated charge is = $0.00843 / 0.06\text{Vs}^{-1}$

$$= 0.1405 \text{ As}$$

$$= 0.1405 \text{ C}$$

The number of electron transferred is = $0.1405\text{C} / 1.602 \times 10^{-19}$

$$= 87.7 \times 10^{16}$$

Hence,

The surface concentration of Ni-Re participated in OER is = 87.7×10^{16} atoms.

Turnover Frequency (TOF) Calculation for Pre-Studies:

$$\text{TOF} = j \times \text{NA} / F \times n \times \Gamma \dots\dots\dots (\text{S1})$$

Where, j = current density, NA = Avogadro number, F = Faraday constant, n = Number of electrons, Γ = Surface concentration.

i) $4\text{A}/\text{dm}^2$

$$\text{TOF}_{1.6\text{V}} = [(2.48 \times 10^{-3}) (6.023 \times 10^{23})] / [(96485) (4) (36.52 \times 10^{16})]$$
$$= 0.011 \text{ s}^{-1}$$

ii) $8\text{A}/\text{dm}^2$

$$\text{TOF}_{1.6\text{V}} = [(5.84 \times 10^{-3}) (6.023 \times 10^{23})] / [(96485) (4) (45.69 \times 10^{16})]$$
$$= 0.02 \text{ s}^{-1}$$

iii) $10\text{A}/\text{dm}^2$

$$\text{TOF}_{1.6\text{V}} = [(10.89 \times 10^{-3}) (6.023 \times 10^{23})] / [(96485) (4) (52.25 \times 10^{16})]$$
$$= 0.032 \text{ s}^{-1}$$

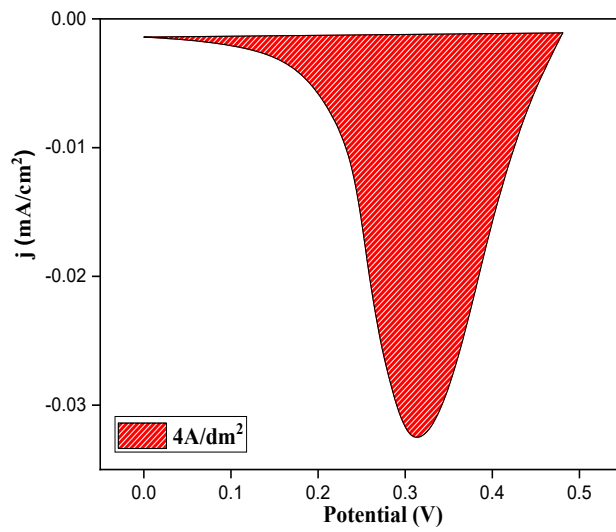
iv) $12\text{A}/\text{dm}^2$

$$\text{TOF}_{1.55\text{V}} = [(17.23 \times 10^{-3}) (6.023 \times 10^{23})] / [(96485) (4) (87.7 \times 10^{16})]$$
$$= 0.031 \text{ s}^{-1}$$

Fig.S10:

Determining Surface concentration from the redox curves of CV's of before activation:

i) $4\text{A}/\text{dm}^2$:



S.A-0.00553VA

• **Calculation:**

Calculated area = 0.005553VA

The associated charge is = $0.00553 / 0.06 \text{Vs}^{-1}$

$$= 0.0921 \text{ As}$$

$$= 0.0921 \text{ C}$$

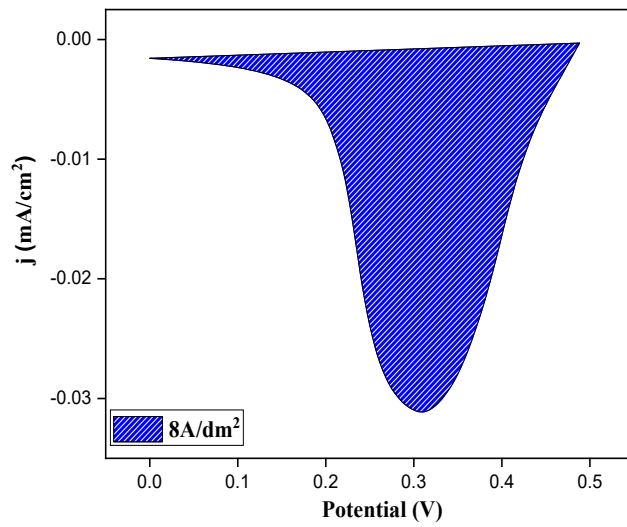
The number of electron transferred is = $0.0921 \text{C} / 1.602 \times 10^{-19}$

$$= 57.49 \times 10^{16}$$

Hence,

The surface concentration of Ni-Re participated in OER is = 57.49×10^{16} atoms.

ii) **8A/dm²:**



S.A-0.00553VA

• **Calculation:**

Calculated area = 0.00595VA

The associated charge is = $0.00595 / 0.06 \text{Vs}^{-1}$

$$= 0.0992 \text{ As}$$

$$= 0.0992 \text{ C}$$

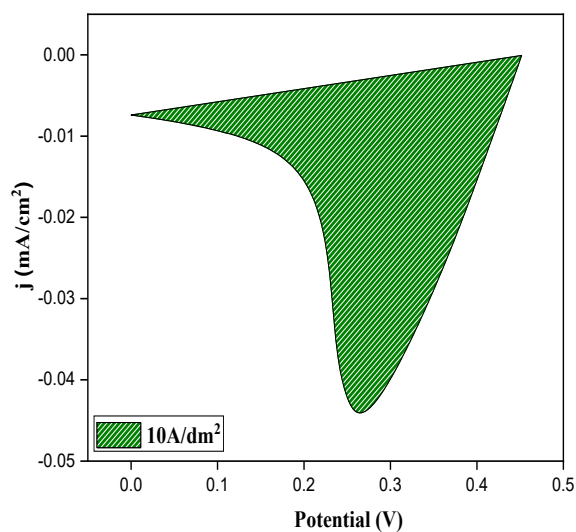
The number of electron transferred is = $0.0992 \text{C} / 1.602 \times 10^{-19}$

$$= 61.92 \times 10^{16}$$

Hence,

The surface concentration of Ni-Re participated in OER is = 61.92×10^{16} atoms.

iii) **10A/dm²:**



S.A-0.00869VA

- **Calculation:**

Calculated area = 0.00869VA

The associated charge is = $0.00869 / 0.06 \text{Vs}^{-1}$

$$= 0.1448 \text{ As}$$

$$= 0.1448 \text{ C}$$

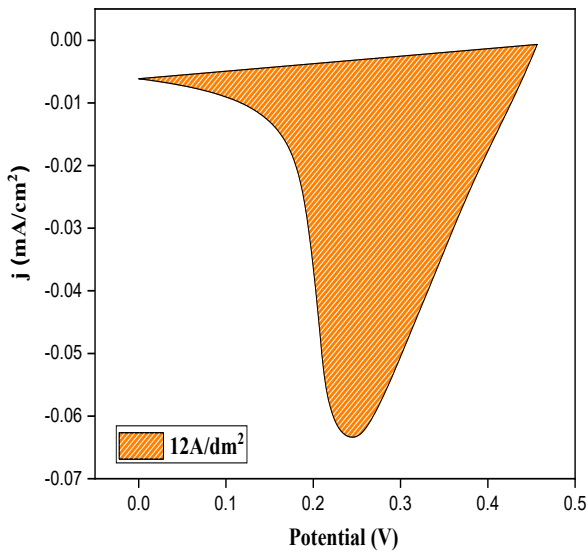
The number of electron transferred is = $0.1448 \text{C} / 1.602 \times 10^{-19}$

$$= 90.39 \times 10^{16}$$

Hence,

The surface concentration of Ni-Re participated in OER is = 90.39×10^{16} atoms.

iv) **12A/dm²:**



S.A-0.01193VA

• **Calculation:**

Calculated area = 0.01193VA

The associated charge is = $0.01193 / 0.06 \text{Vs}^{-1}$

$$= 0.1988 \text{ As}$$

$$= 0.1988 \text{ C}$$

The number of electron transferred is = $0.1988 \text{C} / 1.602 \times 10^{-19}$

$$= 124.09 \times 10^{16}$$

Hence,

The surface concentration of Ni-Re participated in OER is = 124.09×10^{16} atoms.

Turnover Frequency (TOF) Calculation for Post Studies:

i) **4A/dm²**

$$\text{TOF}_{1.6\text{V}} = [(7.08 \times 10^{-3}) (6.023 \times 10^{23})] / [(96485) (4) (57.49 \times 10^{16})]$$

$$= \mathbf{0.019 \text{ s}^{-1}}$$

ii) **8A/dm²**

$$\text{TOF}_{1.6\text{V}} = [(10.39 \times 10^{-3}) (6.023 \times 10^{23})] / [(96485) (4) (61.92 \times 10^{16})]$$

$$= 0.026 \text{ s}^{-1}$$

iii) $10\text{A}/\text{dm}^2$

$$\text{TOF}_{1.6\text{V}} = [(21.15 \times 10^{-3}) (6.023 \times 10^{23})] / [(96485) (4) (90.39 \times 10^{16})]$$
$$= 0.037 \text{ s}^{-1}$$

iv) $12\text{A}/\text{dm}^2$

$$\text{TOF}_{1.6\text{V}} = [(38.98 \times 10^{-3}) (6.023 \times 10^{23})] / [(96485) (4) (124.09 \times 10^{16})]$$
$$= 0.049 \text{ s}^{-1}$$

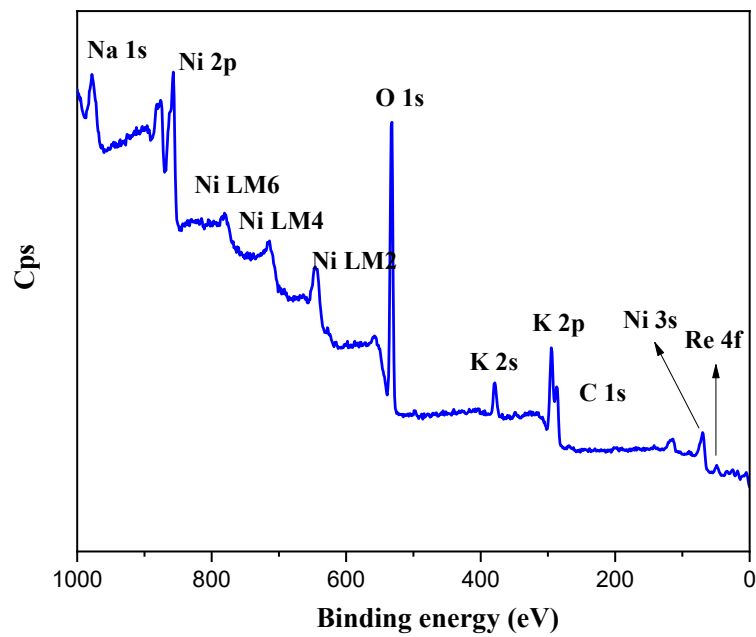


Fig.S11 XPS survey spectra of NR₁₅ alloy after activation.

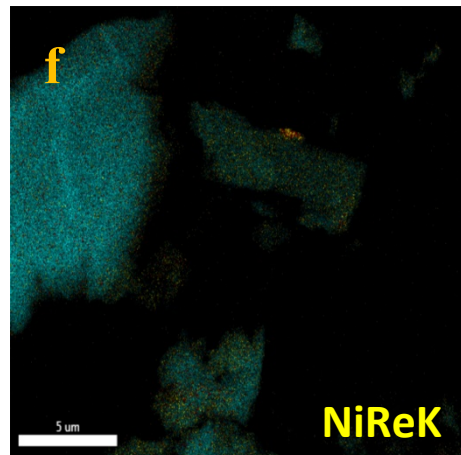
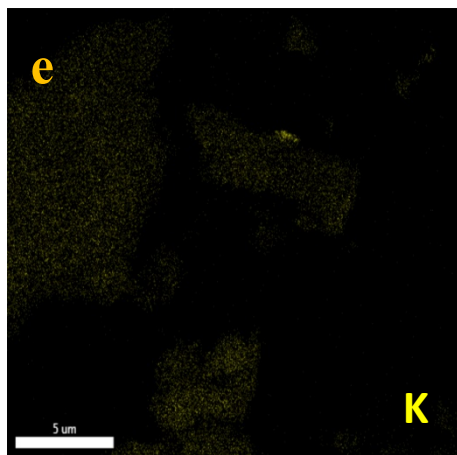
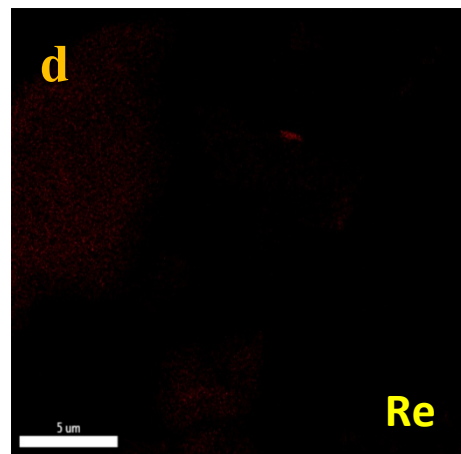
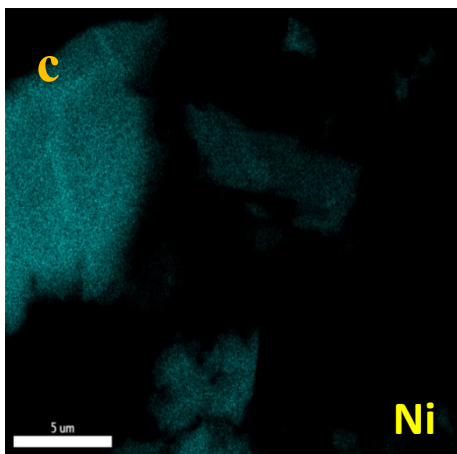
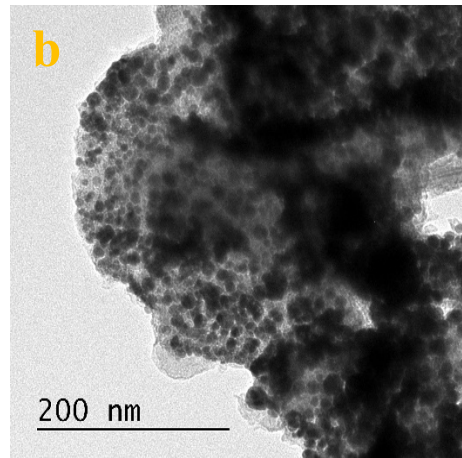
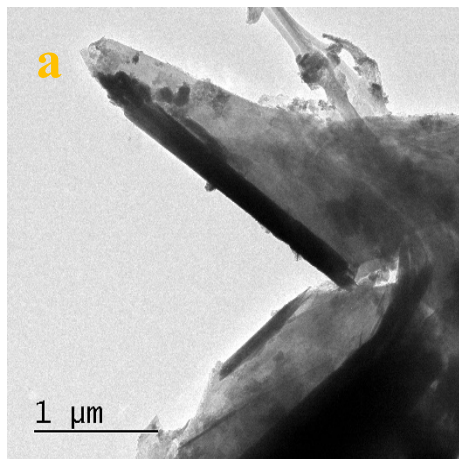


Fig.S12 (a&b) High and low magnification of HR-TEM images of NR₁₅ alloy. Color mapping of c) Nickel, d) Rhenium, e) Potassium f) NiReK.

Crystallite Size Calculation via the Scherrer Equation

$$\mathbf{D = K\lambda / \beta \cos\theta}$$

Where,

D is the crystalline size,

K is the shape factor,

λ is the X-ray wavelength (Cu K α =1.5406 Å),

β is the full width at half maximum (FWHM) of the diffraction peak (in radians),

and θ is the Bragg angle (in degrees).

Furthermore, we have explicitly stated that the crystalline size calculation was performed using the diffraction peak corresponding to the (011) plane of NiRe, which ensures unambiguous reporting of our results.

The calculation method for d-spacing values.

To improve clarity, we included the d-spacing values that were calculated using Bragg's law:

$$\mathbf{d = n\lambda / 2 \sin \theta}$$

Where:

d is the interplanar spacing,

n is the diffraction order,

λ is the X-ray wavelength,

θ is the Bragg angle.

The lattice strain in our study was calculated using the Williamson-Hall (W-H) method, specifically the uniform deformation model. The equation used is derived from:

$$\mathbf{\beta \cos \theta = k\lambda / D + 4 \epsilon \sin \theta}$$

ϵ is the lattice strain,

β is the full width at half maximum (FWHM) of the diffraction peak

θ is the bragg angle corresponding to the main diffraction peak.

λ is the X-ray wavelength (typically 1.5406 Å for Cu K α),

D is the crystalline size,

And k is the shape factor (commonly taken as 0.9).

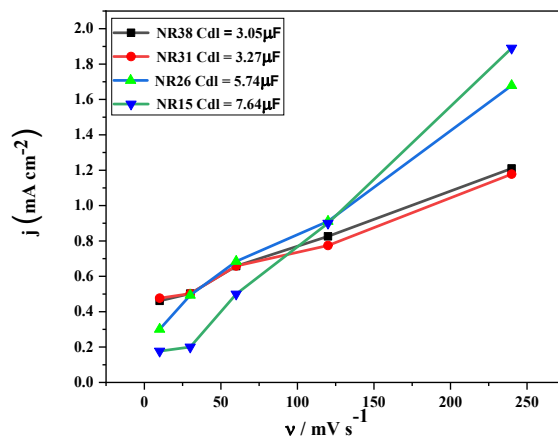
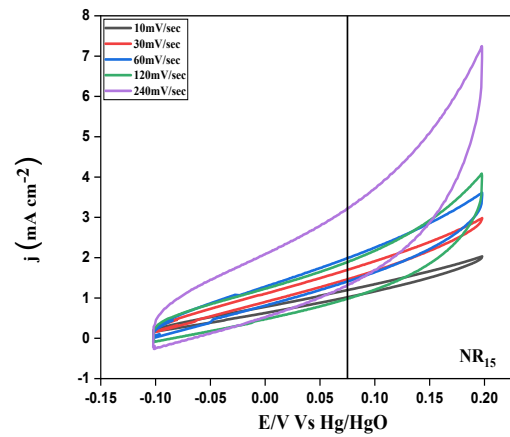
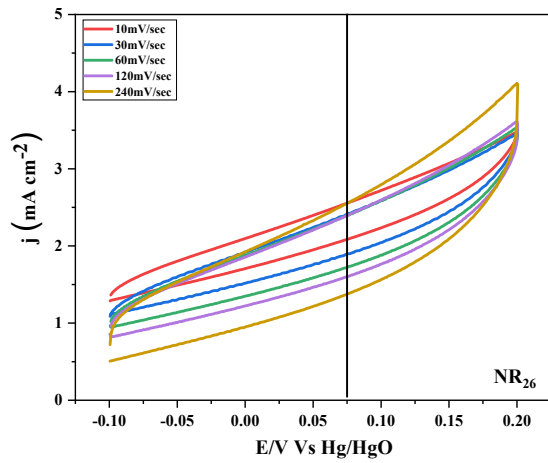
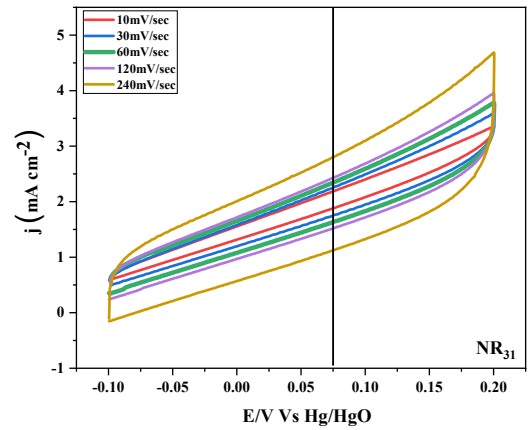
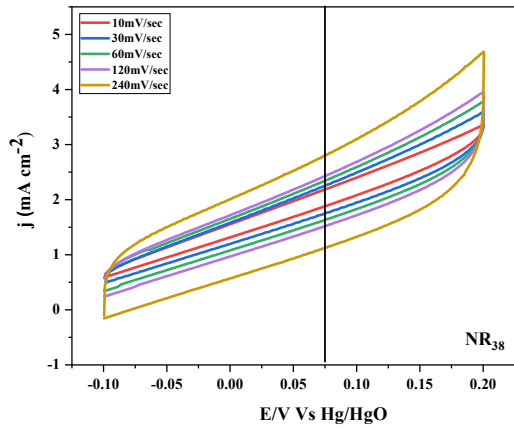
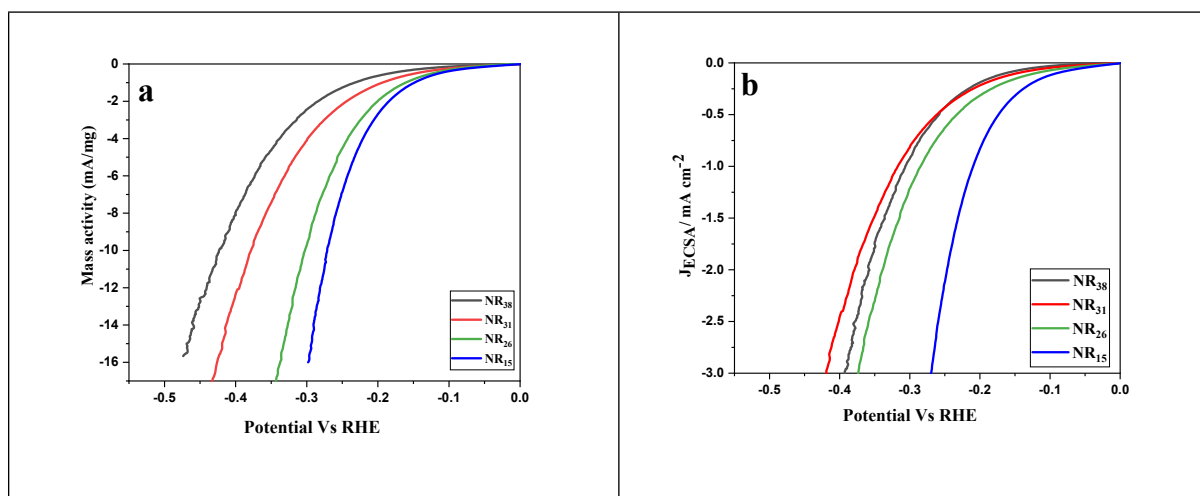


Fig.S13 Calculated Cdl values of a) NR₃₈, b) NR₃₁, c) NR₂₆, d) NR₁₅.



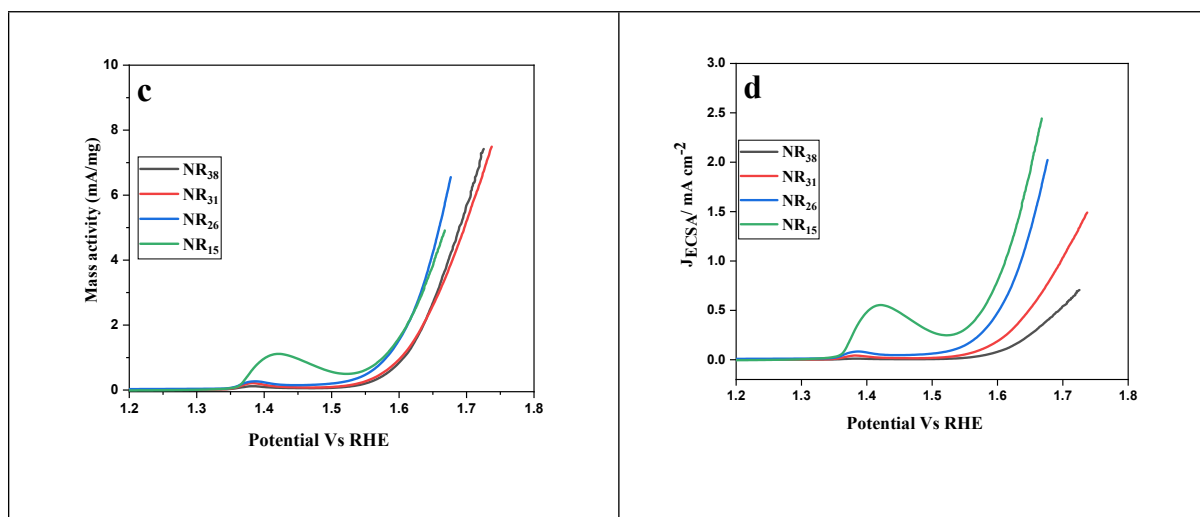


Fig.S14. a) Mass- Normalisation for HER b) Mass- Normalisation of OER c) Electrochemical-Normalisation of HER d) Electrochemical-Normalisation of OER.

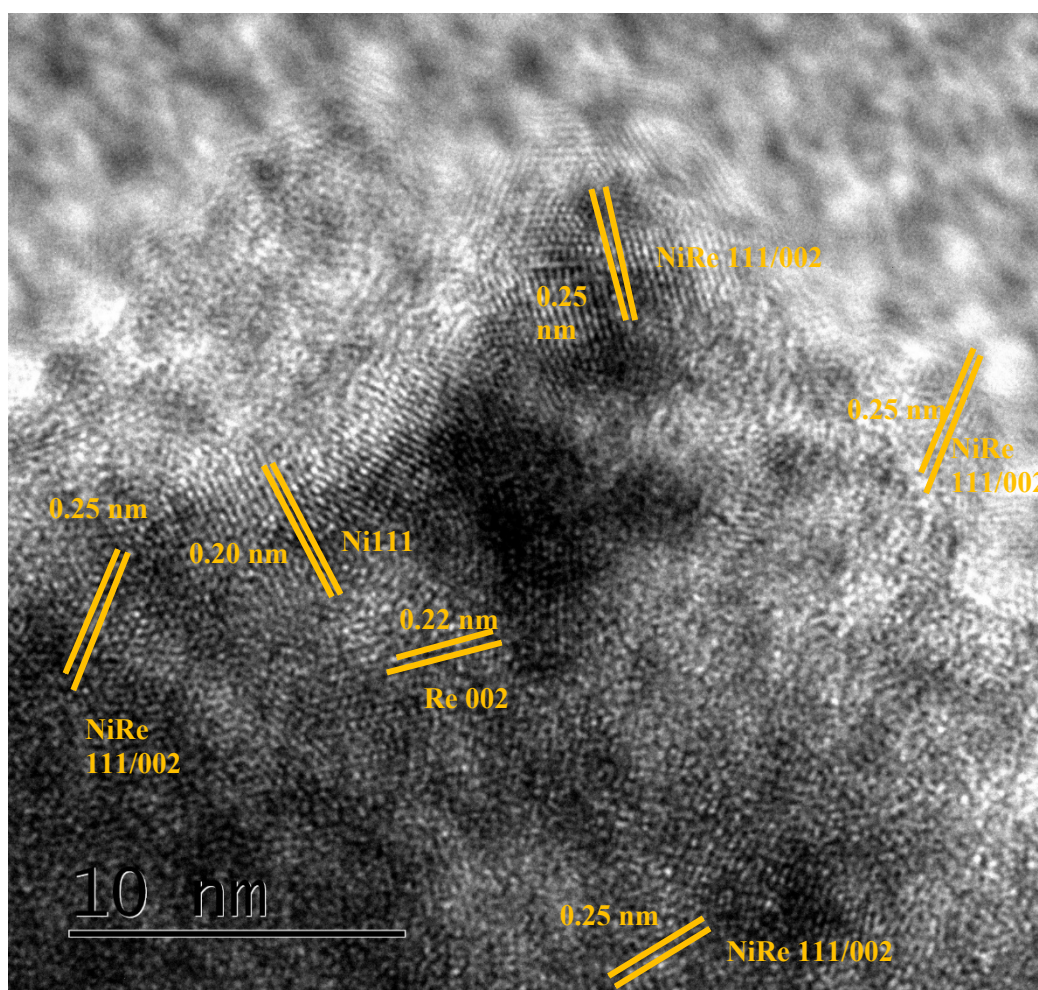


Fig.S15. Lattice fringes of NR₁₅ after electrochemical activation.

References:

- 1 E. Hatami, A. Toghraei and G. Barati Darband, *International Journal of Hydrogen Energy*, 2021, **46**, 9394–9405.
- 2 S. Shetty and A. C. Hegde, *Metallurgical and Materials Transactions B*, 2017, **48**, 632–641.
- 3 A. R. Shetty and A. C. Hegde, 2018, p. 020108.
- 4 R. M. Neethu and A. C. Hegde, *Physica B: Condensed Matter*, 2020, **597**, 412359.
- 5 G. Huang, Z. Xiao, R. Chen and S. Wang, *ACS Sustainable Chemistry & Engineering*, 2018, **6**, 15954–15969.
- 6 Y. Yao, S. Hu, W. Chen, Z.-Q. Huang, W. Wei, T. Yao, R. Liu, K. Zang, X. Wang, G. Wu, W. Yuan, T. Yuan, B. Zhu, W. Liu, Z. Li, D. He, Z. Xue, Y. Wang, X. Zheng, J. Dong, C.-R. Chang, Y. Chen, X. Hong, J. Luo, S. Wei, W.-X. Li, P. Strasser, Y. Wu and Y. Li, *Nature Catalysis*, 2019, **2**, 304–313.
- 7 W. Cheng, X. Zhao, H. Su, F. Tang, W. Che, H. Zhang and Q. Liu, *Nature Energy*, 2019, **4**, 115–122.
- 8 Q. Ji, Y. Kong, C. Wang, H. Tan, H. Duan, W. Hu, G. Li, Y. Lu, N. Li, Y. Wang, J. Tian, Z. Qi, Z. Sun, F. Hu and W. Yan, *ACS Catalysis*, 2020, **10**, 5691–5697.
- 9 D. Voiry, H. Yamaguchi, J. Li, R. Silva, D. C. B. Alves, T. Fujita, M. Chen, T. Asefa, V. B. Shenoy, G. Eda and M. Chhowalla, *Nature Materials*, 2013, **12**, 850–855.
- 10 W. Han, Z. Liu, Y. Pan, G. Guo, J. Zou, Y. Xia, Z. Peng, W. Li and A. Dong, *Advanced Materials*, , DOI:10.1002/adma.202002584.
- 11 T. Ling, D.-Y. Yan, H. Wang, Y. Jiao, Z. Hu, Y. Zheng, L. Zheng, J. Mao, H. Liu, X.-W. Du, M. Jaroniec and S.-Z. Qiao, *Nature Communications*, 2017, **8**, 1509.
- 12 J. R. Petrie, H. Jeen, S. C. Barron, T. L. Meyer and H. N. Lee, *Journal of the American Chemical Society*, 2016, **138**, 7252–7255.
- 13 D. Y. Hwang, K. H. Choi, J. E. Park and D. H. Suh, *Physical Chemistry Chemical Physics*, 2017, **19**, 18356–18365.

